NATIONAL ADVISORY COMMITTEE FOR AERONAUTICS

WARTIME REPORT

ORIGINALLY ISSUED

November 1944 as
Advance Confidential Report 4H24

NACA WR W90

INVESTIGATION OF THE BEHAVIOR OF PARALLEL TWO-DIMENSIONAL AIR JETS

By Stanley Corrsin
California Institute of Technology

NACA

WASHINGTON

NACA ACR No. 4H24

NATIONAL ADVISORY COMMITTEE FOR AERONAUTICS

[redacted] REPORT

INVESTIGATION OF THE BEHAVIOR OF PARALLEL TWO-DIMENSIONAL AIR JETS

By Stanley Corrsin

SUMMARY

An investigation was made of the flow downstream from a "two-dimensional" grid, formed of parallel rods. The two-dimensional character of the flow was insured by end plates normal to the rods and covering the entire flow field.

The jets issuing from between the rods were found to be unstable for the grid density used $\left(\lambda = \frac{\text{covered area}}{\text{total area}} = 0.83\right)$, and possible methods of stabilizing the flow were investigated. Stability was achieved by two methods: (1) by the installation of a high-resistance, fine-mesh damping screen downstream from the rods within a certain range of positions; (2) by means of a large lateral contraction immediately downstream from the rods. Doubling of the initial turbulence in the jets coming from between the rods had no noticeable effect on the flow.

The nature of the flow was determined primarily by means of total-head measurements. Provision was made for heating the rods; and temperature distributions were measured in the unstable and the screen-stabilized configurations. Turbulence level distributions were also measured in the latter case.

Preliminary tests were made in both the closed-duct and the open, two-dimensional configurations; but it was found that the same phenomenon occurred in both cases; so no side walls were used in the setup for the final measurements.

INTRODUCTION

It is known that under certain conditions, not yet established quantitatively, the flow downstream from a grid is unstable. The instability results in a rapid amalgamation of adjacent jets issuing from the open parts of the grid.

In order to simplify the investigation of this phenomenon, a field of parallel two-dimensional jets was used rather than a field of three-dimensional jets, such as would occur behind a conventional square mesh grid.

There is, of course, no basic difference between a field of parallel two-dimensional jets and a field of parallel two-dimensional wakes. It is the usual convention, when the flow field in question has been set up by a grid made of one row of parallel rods in an air stream, to describe this field as composed of jets if the grid density is high, and of wakes if the grid density is low. The grid density, or solidity, is defined as the ratio of blocked area to total area.

Apparently the first published systematic measurements behind a row of rods were made by R. Gran Olsson (reference 1) in 1936. However, his grid densities were small ($\lambda_{max} = 0.25$) and in addition, his mean flow was not kept two-dimensional since there were no end plates normal to the rods to prevent inflow parallel to the rods. The maximum jet aspect ratio was 33. Thus, he found no instability, and, in fact, he was concerned only with the problem of mixing in fully developed turbulent flow.

G. Cordes (reference 2) investigated essentially the same problem as Gran Olsson, and met with no instability for the same two reasons.

Both of these investigators presented theoretical solutions for the (stable) fully turbulent flow behind parallel rods, based on the momentum transfer theory, with Prandtl's suggested extended assumption for the exchange coefficient (reference 3), involving the use of two mixing lengths. Later, T. Okaya and M. Hasegawa (reference 4) elaborated somewhat on the Gran Olsson and Cordes theoretical analyses.

As far as can be determined, experimental evidence of the occurrence of instability behind, effectively, a row of rods, was first published by D. C. MacPhail (reference 5) in 1939. MacPhail

was concerned with obtaining uniform flow in a duct which followed a simultaneous 90° bend and sudden expansion. He found that the use of corner vanes alone resulted in chaotic flow downstream when the vanes were relatively close together. Then he observed that the introduction of a fine-mesh, high-resistance screen downstream from the vanes resulted in considerably improved flow. However, MacPhail apparently did not interpret the phenomenon as a stability problem.

In 1940, J. G. von Bohl (reference 6) published the results of measurements in the flow behind rod grids in a closed duct. He was specifically concerned with the stability of the flow and, by sufficient variation of the grid density, succeeded in obtaining both stable and unstable cases. He made no attempt to stabilize the normally unstable flow. In the same paper, he presented an analysis based on the small perturbation method, which gave qualitatively the correct result, that is, that the degree of stability decreases with increasing grid density.

Bohl's analysis began with a sinusoidal velocity distribution in the main flow, and a small superimposed sinusoidal disturbance of wave length considerably longer than the original. Working with the first two equations of motion, he effectively assumed the exchange coefficient $\epsilon \sim \frac{1}{x}$ and used the extended Prandtl form of ϵ (reference 3). After several coordinate transformations he obtained an ordinary differential equation of fourth order for the amplitude of the disturbance function. This could be solved by a series which unfortunately diverged in the neighborhood of the grid. Therefore, he divided the x-axis into a series of sections, taking the coefficients of the equation constant over each section, and obtained exponential solutions for each section. He then carried out the theoretical calculations for two of the grids tested, and got a qualitative check between theory and experiment.

Although the physical justifications for some of Bohl's simplifications are not clear, the analysis is worthy of notice as the first one published on this problem, and because the results are indicative at least of a possible method of attack.

The matter of flow stability behind a grid is of importance in several practical problems. The applicability to heat exchangers is obvious. Corner vanes in ducts or wind tunnels, especially with

simultaneous turning and expansion, may cause instability, as illustrated in MacPhail's experiments. Furthermore, the flow behind slatted dive brakes on an airplane may also be subject to this type of instability, and may be associated with severe aileron or tail buffeting.

The present investigation, conducted at the California Institute of Technology, was sponsored by, and conducted with financial assistance from, the National Advisory Committee for Aeronautics. The work was carried out under the general supervision of Dr. Th. von Kármán and Dr. C. B. Millikan, whose interest is gratefully acknowledged. Particular thanks are due to Dr. Hans W. Liepmann for his invaluable advice throughout the research.

SYMBOLS

x distance in direction of tunnel axis, measured from plane of rod faces

y lateral distance parallel to rod faces and perpendicular to slots, measured from tunnel center line

z lateral distance in slot direction

U axial component of mean velocity (with respect to time)

u axial component of instantaneous velocity fluctuation

$u' = \sqrt{\overline{u}^2}$

$\frac{u'}{U}$ turbulence level

H total head

λ grid density $= \frac{\text{covered area}}{\text{total area}}$

T temperature, $^{\circ}C$

EQUIPMENT

Aerodynamic Setup

The wind tunnel used in this investigation is essentially the same unit as was used in previous tests on a single axially symmetrical jet (reference 7). Figure 1 is a schematic diagram, approximately to scale, of the tunnel as modified. The principal difference is the installation of the new "nozzle plate" to give a row of seven parallel two-dimensional jets. An enlarged cross-sectional view of the nozzle plate, which is constructed of a row of brass rods, is given in the same figure, as well as a dimensioned cross section of a single rod. Although the aspect ratio of the slots is 40 (8 by 0.2 in.), it was found that end plates (dotted in fig. 1) over the field of flow were nevertheless necessary for maintenance of the two-dimensional character of the mean flow. The two-dimensionality was checked in both stable and unstable cases by a comparison of traverses made at different y-positions. Figures 2 and 3 show the unmounted nozzle plate photographed from the upstream side. Figure 4 is an over-all view of the tunnel from the downstream end, showing the end plates, the motor-driven traversing screw (details in reference 7), and the damping screen near the nozzle plate. Figure 5 is a close-up showing the screen mounting more clearly, as well as the end plates and the fine total-head tube. The nozzle plate can be seen through the screen, which is at $x = 1\frac{1}{4}$ inches in this figure. The rubber tubing on the right carries the tunnel reference static pressure.

The brass rods can be heated electrically to permit a comparison of downstream temperature distributions in the unstable and the stabilized cases.

One method of stabilizing the flow was the introduction of a high-resistance, fine-mesh (65 per in.) damping screen a small distance away from the face of the nozzle plate (fig. 5). The screen extends laterally well into the region of stationary air on both sides of the jet system. The screen is made of rayon, and its degree of regularity can be judged from the center of figure 18A; lens aberration has distorted the edges of the field appreciably. The thread diameter averages 0.004 inch, giving a screen density of 0.52. The closed-duct resistance coefficient, computed from the results of Eckert and Pflüger (reference 8), is $\frac{\Delta p}{q} = 3.0$.

This coefficient is the ratio of the pressure drop in the air passing through a section of the screen stretched across a closed duct, divided by the dynamic pressure of the flow. In a free jet, with essentially the same static pressure at some distance on both sides of the screen, the loss of dynamic pressure through the screen was about 90 percent of the initial dynamic pressure, at least in the low-speed range used in this investigation.

In the case of a single free circular jet passing through the damping screen placed about in the plane of the vertex of the potential cone, where the jet begins to approach the "fully developed" condition, the increase in width was on the order of 60 percent; the characteristic lateral dimension chosen was the diameter of the circle on which the velocity was half the maximum value at the section. However, with the screen placed at a section well into the potential cone (e.g., at $x = r$, the radius of the nozzle mouth) the spread was only about 20 percent.

Provision was made for the installation of straight vertical side walls between the end plates, but preliminary runs showed that the flow phenomena were identical in the closed-duct configuration and the two-dimensional free jet configuration; therefore all final tests were run with the latter, more convenient, arrangement.

A typical section of the downstream contraction used to stabilize the flow is sketched in figure 1. The two rigidly curved walls, circular arcs of 11½-inch radius, were hinged at the edges of the nozzle plate to permit free adjustment of throat size.

Measuring Equipment

Total-head measurements were the principal means of investigating the behavior of the flow. Both total head and temperature were photographically recorded, using a hypodermic needle total-head tube and a copper-constantan thermocouple, respectively. The auxiliary equipment, including automatic traversing unit, is described in reference 7. The average traversing time was 20 minutes.

In many of the total-head distributions, negative readings are recorded. These are, of course, regions of lateral or of reversed flow, the former being of more frequent occurrence. Figure 6 is a directional calibration of the total-head tube.

The level of the turbulence in the mean-flow direction also was recorded by the continuous photographic method, using the light beam reflected from a wall galvanometer to the moving sensitized paper. The hot-wire anemometry equipment is described in reference 7.

Since each turbulence level traverse was run continuously, it was necessary to use an average of the correct values of resistance in the compensation circuit of the amplifier. In order to get a measure of the error introduced by this method, one segment of a turbulence-level distribution was also run with the conventional point-by-point procedure. The results of the two methods, given in figure 7, show surprisingly little divergence. This is because the hot wire was run at the relatively low average temperature difference of about 75° C above room temperature.

Some preliminary measurements of flow direction were made; the instrument employed was a small rotatable unit carrying a heated wire, and a thermocouple connected to a galvanometer (fig. 8). At each test point in the flow, this unit is rotated until the position of maximum galvanometer deflection is reached, corresponding to a thermocouple position in the center of the heated wire wake. The angle is measured electrically with the help of a small rheostat mounted directly on the instrument. However, no extensive direction surveys were carried out since the results did not justify the time necessary for such measurements.

MEASUREMENTS

Unless otherwise described, all measurements were made with unheated rods and with the two-dimensional open-jet configuration; that is, with end plates but without side walls. The following principal measurements are included in the report:

1. Total-head distributions at a series of x-positions in the normal unstable flow. These show the combining of adjacent jets.

2. Flow-direction traverses at given x-positions in the unstable flow, which also show the combining of adjacent jets.

3. A series of total-head distributions with the end plates removed, to illustrate the effect of permitting entrainment of air into the "dead air" regions between jets.

4. A series of total-head distributions with the stabilizing screen in different representative positions, to demonstrate its effect. In each case, traverses were made at a series of x-stations downstream from the screen.

5. Simultaneous turbulence-level and total-head distributions at a series of x-stations in a typical screen-stabilized flow.

6. Total-head distributions at the throats of various side wall contractions (closed duct arrangement), downstream from the rods, to show the effect of immediate contraction on the stability of the system.

7. Simultaneous temperature and total-head distributions at a series of x-stations in the unstable case with heated rods, to give a comparison of the spread of heat and of momentum.

8. Simultaneous temperature and total-head distributions at a series of x-stations in a typical screen-stabilized case with heated rods, to give a comparison of the spread of heat and of momentum, and to contrast with the unstable case.

RESULTS

In general, the experimental results presented in this report are qualitative rather than quantitative, in that no attempt has been made to correct the numerical values for disturbing effects, although the measurements have been made carefully. Specifically, the total-head readings were affected by both turbulence level and variations in mean-flow direction, and hot-wire readings of turbulence level probably began to lose accuracy for $\frac{u'}{U}$ greater than about 20 percent (reference 7, appendix).

Since this was principally a phenomenological study, the air velocities were chosen for convenience of recording. Except where a different value is specifically given in the text, all runs without damping screen were made with a tunnel reference pressure (upstream from the rods) of 0.095 pound per square foot, while all runs with the screen in place were made at a reference pressure of 0.380 pound per square foot.

The rods were heated only for runs in which temperature measurements were made. A comparison of the total-head traverses taken with and without heat shows no appreciable difference in the flow. Also, the resulting air density variations are apparently negligible in their effect on the reading of total head. Turbulence level was measured with the rods unheated since temperature fluctuations would affect the hot-wire output.

The principal experimental result was the observed instability of the system of two-dimensional jets issuing from the slots in a grid made up of a row of parallel rods, with a grid density of 0.83. The instability consisted of a grouping together of adjacent jets immediately after their exit from the slots, resulting in wildly eddying flow. Adjacent groups then joined, and at a very short distance from the nozzle plate, the flow was no longer identifiable as having originated from a regular row of slots. The phenomenon was nonstationary in the sense that the same pairs of adjacent jets did not always unite first. This fact shows that the phenomenon was not caused by mechanical imperfections in the nozzle plate. Fortunately, a single flow configuration usually was maintained for a long enough time to permit at least one traverse, and often for considerably longer.

Figure 9 is a series of lateral total-head traverses at different downstream distances, for the same flow configuration (reference pressure = 0.285 lb/sq ft). In this case, the flow started out as seven uniform, equally spaced jets (for $x = 1/2$ in., see, for instance, fig. 19). Almost immediately, jet 1 combined with jet 2, jet 3 with jet 4, and jets 5 and 6 with jet 7 (fig. 9C). Then, jet 1 - 2 combined with jet 3 - 4 (fig. 9D); and finally, jet 1-2-3-4 joined jet 5-6-7 (fig. 9F). At $x = 10$ inches, the flow looked as if it had originated from a single jet.

The drawing of the nozzle-plate face is to the same lateral scale as the total-head distributions.

The two recorded alternative flow configurations resulting from the instability are compared in figure 10. It is seen that they were essentially mirror images, one with the two-two-three initial combination groups and the other with three-two-two. The third, symmetrical, possibility, two-three-two, was encountered only once during the investigation, and then only for a part of one traverse.

This prompt joining of adjacent jets naturally involved considerable deviations of individual jets from flow in the direction of the x-axis. Figure 11 gives the results of the direction measurements mentioned previously. The spacing and length of the vectors have no significance; only flow direction is represented. It should be remarked that the traverse at $x = 2$ inches clearly corresponds to the reverse unstable flow configuration from figure 9D.

The jets were partially stabilized by the removal of the end plates, permitting a net flow into the system along the third (z) axis (fig. 12).

Complete stabilization of the flow was achieved by the introduction of a fine-mesh, high-density screen parallel to the face of the nozzle plate and anywhere between 1/4 inch and $1\frac{1}{2}$ inches downstream from it. The screen characteristics are described in the previous section. Figures 13 and 14 show a series of total-head distributions for screen positions in the stabilizing range. All traverses are downstream of the screen. The narrow irregularities that disappear with increasing x are apparently the fine-mesh screen jets in the process of combining with each other. Thus, the screen jet system itself seems to be unstable.

As the damping screen was moved farther than $1\frac{1}{2}$ inches from the nozzle plate or closer than 1/4 inch, the stabilizing effectiveness decreased. Figure 15 is a set of total-head distributions behind the screen placed at $x = 2\frac{1}{8}$ inches. The first traverse was run very close to the damping screen so that the individual screen jets are still distinct.

Setting the screen at $x = 0$, against the face of the rods, had no stabilizing influence on the flow. The principal effect of this arrangement was merely to increase the turbulence level of the jets prior to mixing. The same effect was achieved by introducing a coarse grid (1/8-in. mesh, 1/16-in. wires) into the tunnel 2 inches upstream of the leading edges of the rods. This arrangement also had no noticeable stabilizing influence. Due to the high contraction of the flow passing between the rods, this 1/8-inch grid only doubled the initial turbulence level in the jet potential cones, raising it from 0.30 to 0.55 percent.

The second successful method of stabilizing the field of jets was the installation of a lateral contraction immediately downstream from the rods. The total-head distributions in figure 16 were measured at the throats of three contractions, with area

ratios of 2.0:1, 2.7:1, and 6.7:1. It can be seen that with the highest contraction ratio the center minimum has disappeared, apparently indicating a completely stabilized flow.

In the screen-stabilized flow, the turbulence-level distribution becomes uniform as rapidly as the velocity distribution. The illustrative curves of figure 17 are measurements of the square of the turbulence level, which is the quantity registered by the thermocouple and wall galvanometer combination at the output of the amplifier. Physically, this is a measure at each point of the ratio of fluctuating kinetic energy in the mean-flow direction, to mean-flow kinetic energy. As was to be expected, at small values of x, where the separate jets were still distinguishable, the turbulence maxima coincided with the velocity minima, which were, of course, the mixing regions between jets. The reason for the decreased turbulence level in the mixing regions between jets 1 and 2 and jets 6 and 7 is not evident.

No turbulence-level measurements were made for the free (unstable) jets, since the wildly eddying flow resulting from the instability cannot be regarded as developed random turbulence.

In the course of the investigation it was found that the collecting of dust particles on the damping screen decreased the degree of stability of the downstream flow. The dust was mainly carried in the wind tunnel air stream, and therefore was concentrated on the damping screen in seven narrow strips where the air from the seven slots impinged upon it. Figure 18 shows the effect of screen dust upon the total-head and turbulence distributions. The microphotograph of the dusty screen indicates that the total blocking area of the dust particles was not large. Thus the instability was probably due to the irregularity of the resistance rather than to any increase in the magnitude of the resistance.

Heating the brass rods gave the opportunity for a comparison of temperature distributions corresponding to unstable and stabilized flow, as well as furnishing a comparison of total-head and temperature distribution in each of the two cases. Figures 19 and 20 are traverses in the unstable and the screen-stabilized case, respectively. The rod temperature was lower in the latter case due to higher air velocity, with identical electrical heating in the rods. Since these were cases with cool air blowing past heated rods, the temperature minima coincide with the velocity maxima. In the free jet tests it was possible to get sufficiently close to the nozzle plate to record the temperature maxima in the air that had been in the boundary layers of the rods (fig. 19A). It should be remarked

that the unstable configuration in figures 19A and 19D is opposite to that recorded in 19B and 19C. The temperature distributions in the stable and unstable cases show considerably less contrast than do the corresponding velocity distributions.

Far downstream, measurements in both stable and unstable cases checked the known result, that in a region of turbulent mixing, with temperature differences, the heat spreads more rapidly than the momentum (references 7 and 9).

DISCUSSION

The physical mechanism of this instability of multiple jet systems seems to hinge on the entrainment of air by the individual jets from the dead air regions between them. An hypothesis is as follows: the entrainment reduces the static pressure between jets, tending to force them together. As a jet spreads out downstream, it behaves like a diffuser, so that its center-line static pressure increases downstream. The pressure difference between the jets and the air between them is balanced by divergent curvature of the jet streamlines. Thus, for given air jets, wider spacing requires a relatively greater diffusion angle of the individual jets before adjacent ones touch; and when the spacing is sufficiently great (i.e., for great enough grid density), the necessary angle is prohibitively large, resulting in a breakdown of the flow.

Some very rough static pressure measurements by Bohl indicate a distribution similar to that described.

The present investigation gives no indication of the critical value of grid density, λ_{cr}, and of its possible variations with changes in initial or boundary conditions. Bohl found λ_{cr} between 0.37 and 0.46, the densities for his stable case and minimum-density unstable case, respectively. His grids were made up of flat, sharp-edge wooden slats set normal to the air stream, and λ_{cr} may be a function of rod shape, and also a function of rod Reynolds number.

The limiting case of $\lambda = 0$ corresponds to a uniform flow with no obstruction, and is, of course, stable. The other limit, $\lambda \rightarrow 1.0$, can be approached either by decreasing the spacing of given rods or by increasing the spacing between given jets. If the jet velocity is fixed as λ approaches unity, presumably well

above λ_{cr}, the system would probably remain basically unstable in both cases, although a long time would be required for the entrainment of sufficient air to cause the necessary pressure reduction between the jets. The single two-dimensional jet in an infinite stationary field is, of course, stable.

This type of instability is also to be expected in the field of jets behind a conventional square mesh grid of sufficient density. As pointed out previously, the total-head distributions behind the damping screen clearly show the joining of the small jets. In the flow behind square mesh grids, then, it is to be anticipated that at a given number of mesh lengths downstream the turbulence level should be appreciably higher after an unstable jet system than after a stable system.

A series of measurements of the decay of turbulence behind several grids in a wind tunnel was made several years ago by S. Atsumi at the GALCIT. The mesh sizes varied from 1/8 inch to 1½ inches, and densities from about 0.3 to 0.7. The following table gives the values of $\frac{u'}{U}$ at 75 mesh lengths downstream from the grids. The readings have been corrected approximately for the finite length of the hot wire.

Mesh length, M	Rod diameter, d	Density, λ	Turbulence level at $\frac{x}{M} = 75$, $\frac{u'}{U}$ (percent)
0.50	0.084	0.308	1.33
.50	.105	.376	1.36
1.00	.25	.438	1.33
1.50	.50	.556	1.78
.125	.054	.677	3.11
.50	.23	.708	3.32

This set of values seems to confirm the existence of at least a critical region of λ for the flow behind square mesh grids, between perhaps 0.5 and 0.6. This is somewhat higher than the range found by Bohl for his particular arrangement of rod grids, but there is no reason to anticipate quantitative agreement between the two cases.

The hypothesis that the individual jets act like diffusers is further supported by the experimentally proved possibility of stabilization by means of a downstream damping screen. However, the detailed mechanism of this stabilization is not immediately evident.*

MacPhail (reference 5) also found that it was necessary to install the damping screen a finite distance downstream from the corner vanes in order to get the most uniform resulting flow. He suggested that this gap between vanes and screen was necessary to permit lateral flow for rearrangement of the (supposedly) irregular flow before the screen. However, his velocity measurements indicate greater regularity upstream of the screen than existed at the same region with no screen in the flow. This was also definitely found to be the case in the present investigation.

It should be remarked that MacPhail's set of corner vanes, although made of sheet metal, acted as a high-density grid because they were stalled.

In connection with the attainment of stable flow by means of a contraction, it is interesting to note that for the measured stable case (fig. 16C) the throat area is very nearly equal to the sum of the areas of the seven initial jets. Possibly the amount of contraction necessary to achieve stability is related to the net effective diffusion in going from the sum of the initial jet areas to the throat area.

The fact that an increase of free-stream turbulence level in the jets had no noticeable effect on the stability is not surprising since, in general, turbulent mixing has been found to be independent of the initial turbulence (reference 10, p. 20); and the turbulent mixing at the edges of the jets controls the entrainment of air.

---

*It has been suggested by members of the NACA technical staff that the stabilizing effect of the damping screen may perhaps be attributed to an effective decrease in λ due to forced spreading of the individual jets.

Removal of the end plates did not stabilize the flow completely because of the high aspect ratio of the jets, which tends to keep the flow two-dimensional at the center. In figure 12, although the jet system shows increased over-all regularity as contrasted with the completely unstable case, there exist smaller scale irregularities that were not present in the latter flow. These irregularities arise with the removal of the end plates, and are apparently due to the semistable nature of the flow. They are obviously not random turbulence; the traverses of figure 17, for example, show that the total-head tube does not follow the rapid fluctuations of fully developed turbulent mixing. Thus, these irregularities are actual changes in local mean velocity, probably due to intermittent existence of the stable and the unstable flow configurations. With lower jet aspect ratios, the average flow pattern would probably approach more closely to the completely stable case, while higher jet aspect ratios would lead to a flow more nearly like the completely unstable case of figure 9.

The flow behind slatted airplane dive brakes may be of the type of figure 12 when the slats are built parallel to the wing surface and therefore set up jets of high aspect ratio. Aileron or horizontal tail buffeting appears to be most serious for this arrangement, which is reasonable in view of the orientation of the two-dimensional eddies or vortices arising from the flow instability. This difficulty has been at least partially solved in actual practice by two methods: (1) by the use of a "picket fence" type of slatted dive brake, with the slats perpendicular to the wing surface; this not only rotates the axes of the vortices to a less dangerous orientation, but also permits a decrease in the aspect ratio of the slots between the slats; and (2) by the use of a square mesh grid as a dive brake, thus eliminating the two-dimensional nature of the eddies. The mesh size should be as small as possible in order to give rapid decay of the downstream turbulence developing out of these instability eddies.

Fluctuations downstream of a brake could be reduced by decreasing the solidity to a value below the critical, but high energy losses are desirable; so a combination of high-density grid and downstream damping screen would offer possibilities. However, it is obvious that considerable structural difficulty would be encountered in such an installation. Of course, in heat exchangers and corner-vane installations, on the other hand, it is desirable to keep the losses to a minimum.

It is possible that stabilization by means of a contraction followed by a well-designed diffuser, would involve less total energy loss than an adequate damping screen. In any case, from structural considerations it is evident that the former is more conveniently applicable to dive brakes and to installations where there is a limited available duct length.

Since the present investigation has been principally qualitative, in connection with both the instability phenomenon and the two successful methods of stabilization, there is a great deal of quantitative work to be done.

In general, most of the necessary data would consist of total-head measurements. These can be carried out very conveniently by an automatic traversing and recording arrangement similar to the one used in this investigation. This was set up by Mr. C. Thiele for preliminary measurements in the single axially symmetrical jet (reference 7).

For the stability problem itself, it is suggested that measurements be made with a considerably larger number of parallel jets, and a wide range of grid densities. Also, the possible effect of rod Reynolds number upon the value of the critical grid density should be investigated.

In the matter of screen stabilization, it is of interest to find out the effect of mesh size relative to jet dimensions, as well as the range of damping screen densities which give satisfactory stabilization, with a determination of the optimum density, which, according to results of MacPhail, does exist.

For the method of stabilization by means of a contraction, investigations should be made of the effect of variations in the fundamental geometrical parameters: rate of contraction and total contraction ratio, relative to grid density.

Possible quantitative differences in behavior of three-dimensional and two-dimensional jet fields could be investigated, as well as possible quantitative differences for the latter in the closed-duct and the open-sided cases.

Finally, the range of over-all efficiencies for the two methods of flow stabilization should be determined.

CONCLUSIONS

1. The field of parallel two-dimensional air jets downstream from a grid made up of parallel rods is unstable for a grid density of 0.83. The results of previous investigators show the existence of a critical range of grid density below which the downstream flow is stable and above which it is unstable. The same phenomenon occurs in both two- and three-dimensional jet fields.

2. The flow can be completely stabilized by the introduction of a fine-mesh damping screen parallel to the grid plane and within a definite range of positions downstream from the grid.

3. The flow can be completely stabilized by means of an adequate lateral contraction beginning immediately after the grid.

4. The flow can be at least partially stabilized by the "ventilation" of the spaces between jets, permitting air to flow into the system in the third dimension, parallel to the rod axes.

5. Doubling of the initial turbulence level in the jets has no noticeable effect on the stability.

California Institute of Technology,
Pasadena, Calif., August 1944.

REFERENCES

1. Gran Olsson, R.: Geschwindigkeits- und Temperaturverteilung hinter einem Gitter bei turbulenter Strömung. Z.f.a.M.M., Bd. 16, Heft 5, Oct. 1936, pp. 257-274.

2. Cordes, G.: Untersuchungen zur Statischen Druckmessung in turbulenter Strömung. Ing.-Archiv., Bd. 8, Heft 4, Aug. 1937, pp. 245-270.

3. Prandtl, L.: Bericht über Untersuchungen zur ausgebildeten Turbulenz. Z.f.a.M.M., Bd. 5, April 1925, pp. 136-139.

4. Okaya, T., and Hasegawa, M.: On the Velocity Distribution of Flow behind the Parallel Rods. Japanese Jour. of Phys., vol. 14, Jan. 1941, pp. 1-9.

5. MacPhail, D. C.: Experiments on Turning Vanes at an Expansion. R. & M. No. 1876, British A.R.C., 1939.

6. von Bohl, J. G.: Das Verhalten paralleler Luftstrahlen. Ing.-Archiv, Bd. 11, Heft 4, 1940, pp. 295-314.

7. Corrsin, Stanley: Investigation of Flow in an Axially Symmetrical Heated Jet of Air. NACA ACR No. 3L23, 1943.

8. Eckert, B., and Pflüger, F.: The Resistance Coefficient of Commercial Round Wire Grids. NACA TM No. 1003, 1942.

9. Ruden, P.: Turbulente Ausbreitungsvorgänge in Freistrahl. Die Naturwissenschaften, Bd. 21, Heft 21/23, May 1933, pp. 375-378.

10. Liepmann, Hans W.: Investigations on Laminar Boundary-Layer Stability and Transition on Curved Boundaries. NACA ACR No. 3H30, 1943.

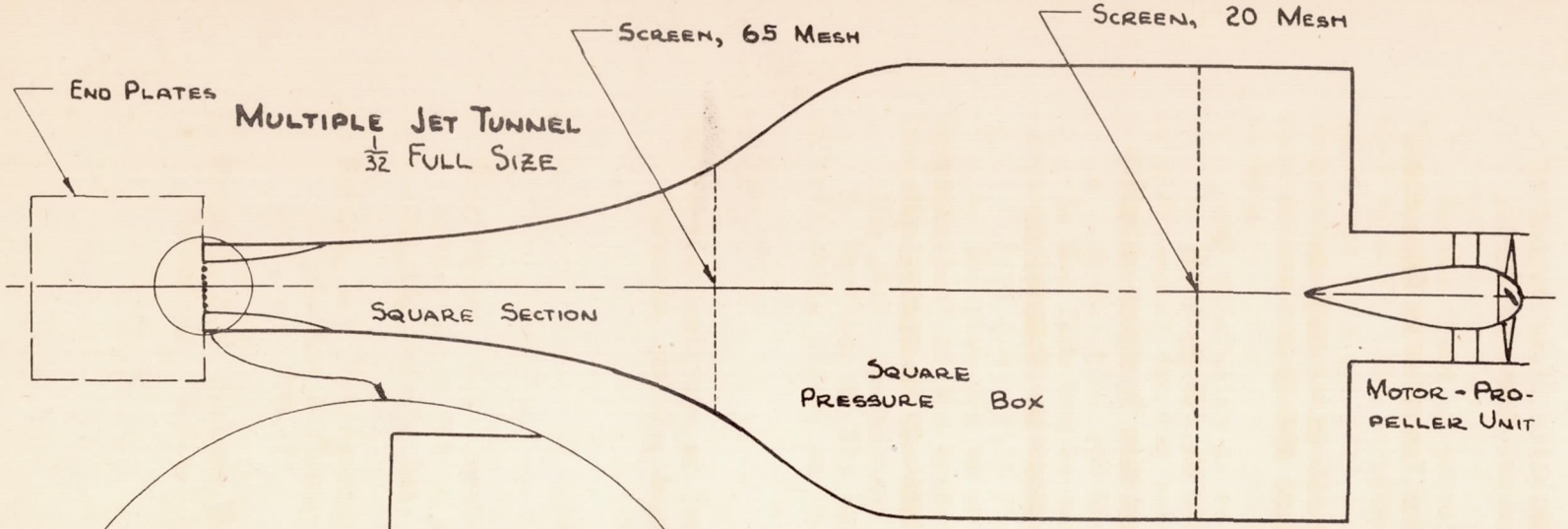

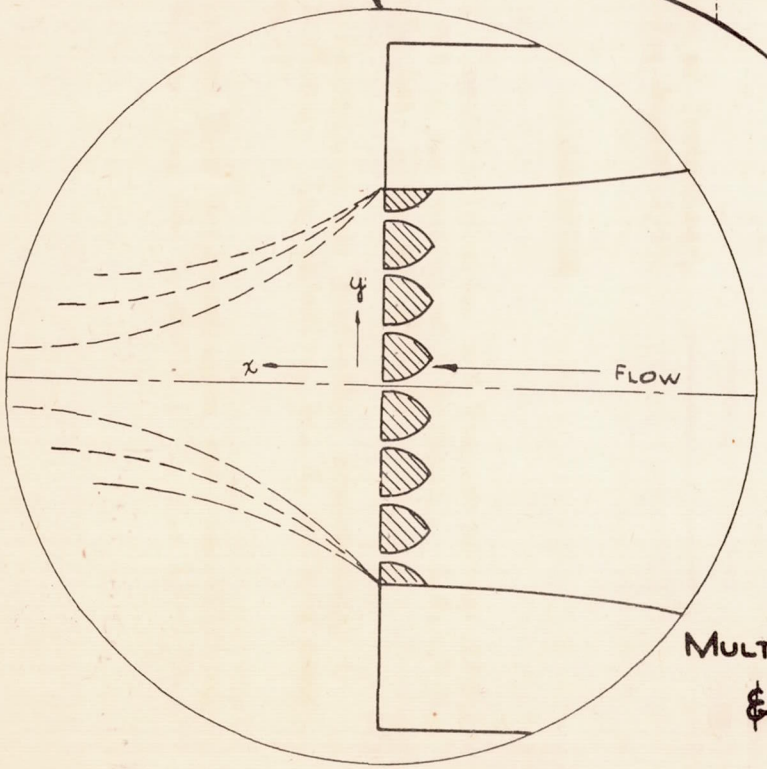

Multiple Jet Unit
& Contractions
1/4 Full Size

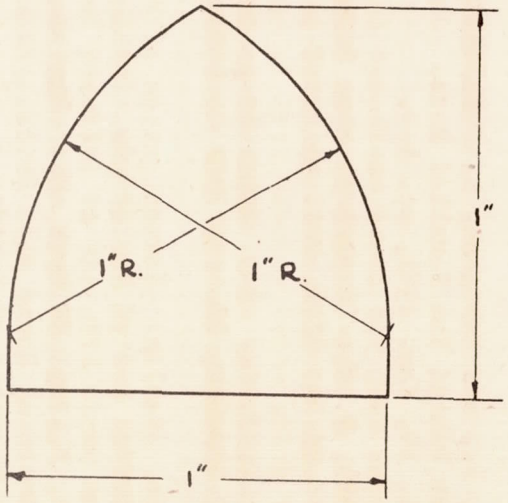

Jet-Forming Rod
Twice Full Size

Figure 1

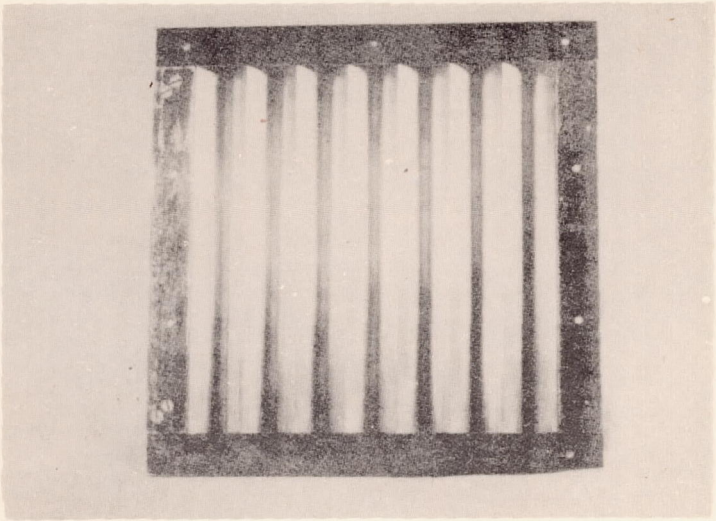

Figure 2.- Nozzle plate; upstream side.

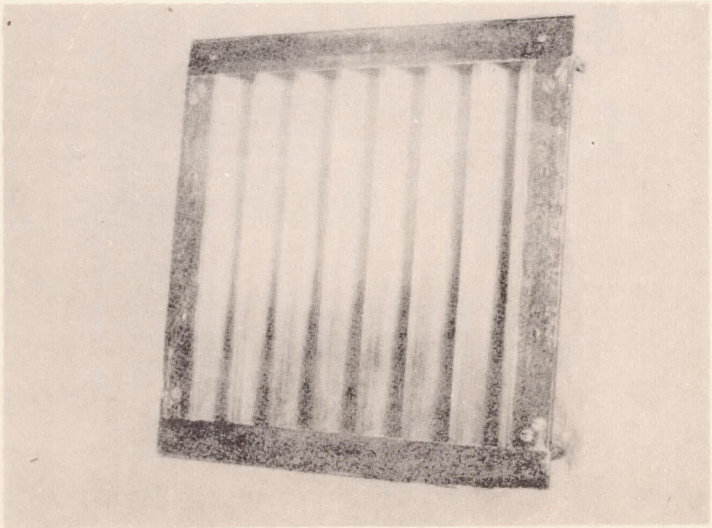

Figure 3.- Nozzle plate; upstream side.

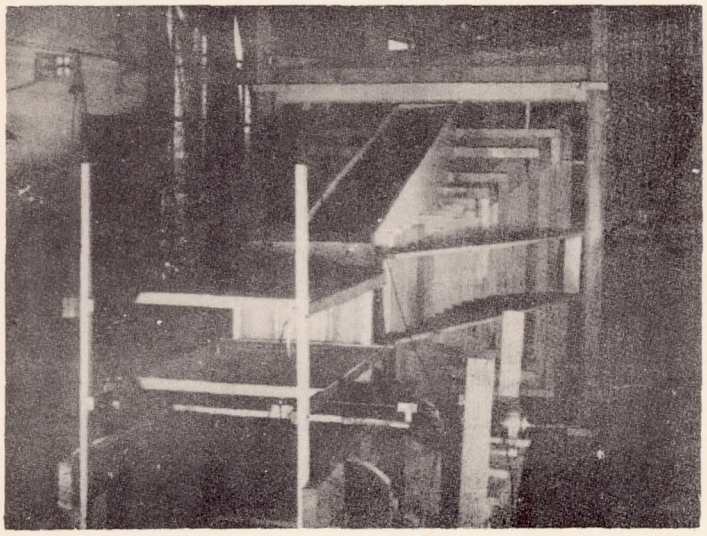

Figure 4.- Tunnel and traversing equipment.

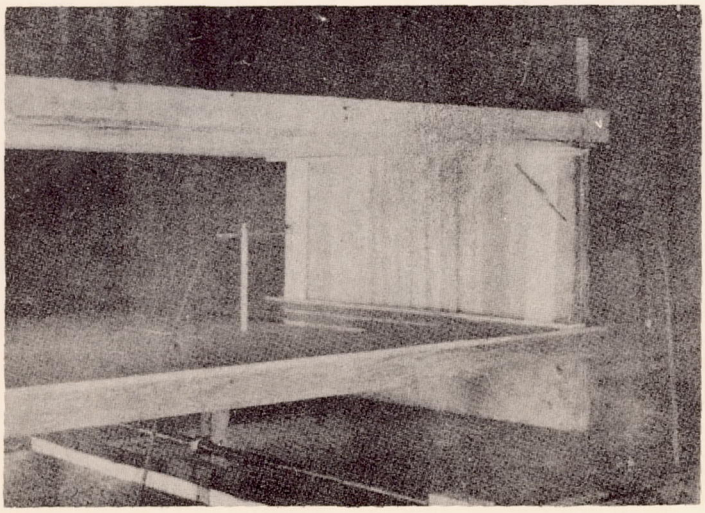

Figure 5.- Flow region; damping screen 1-1/4" downstream of slots. Total head tube in flow.

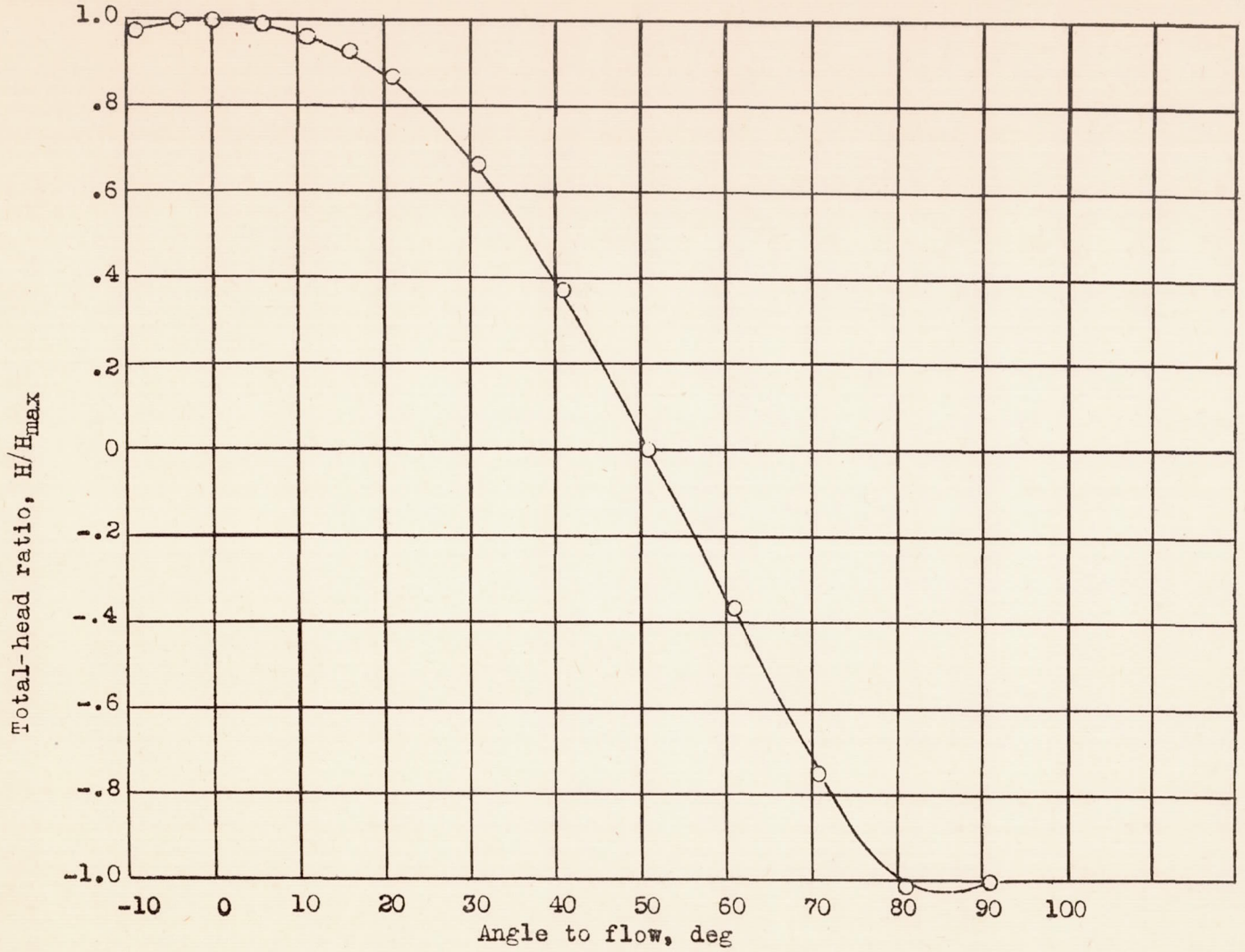

Figure 6.- Total-head tube; directional sensitivity.

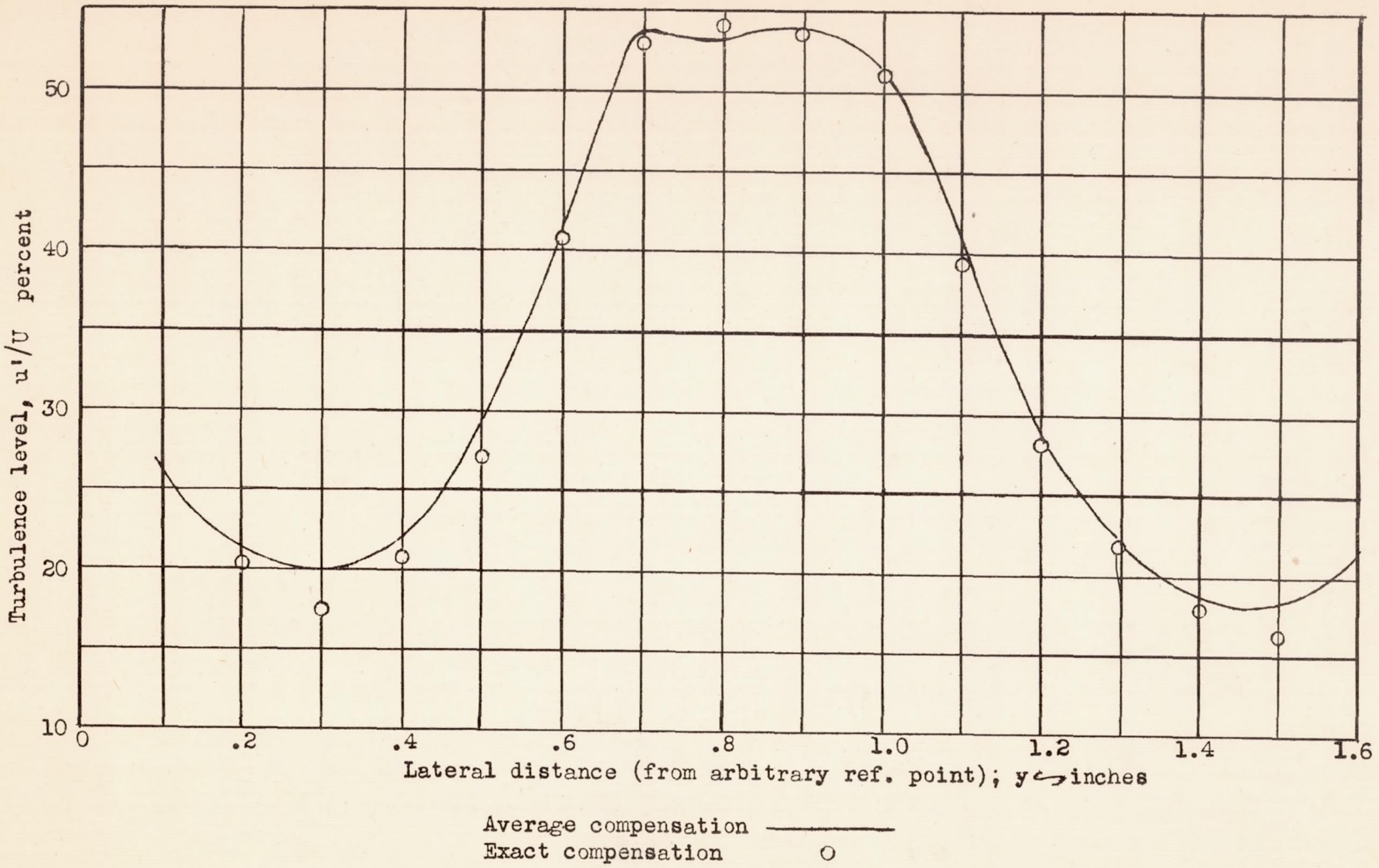

Figure 7.- Effect of using average compensation in turbulence traverse. Section of stabilized flow; x = 2"; screen at 1-1/4".

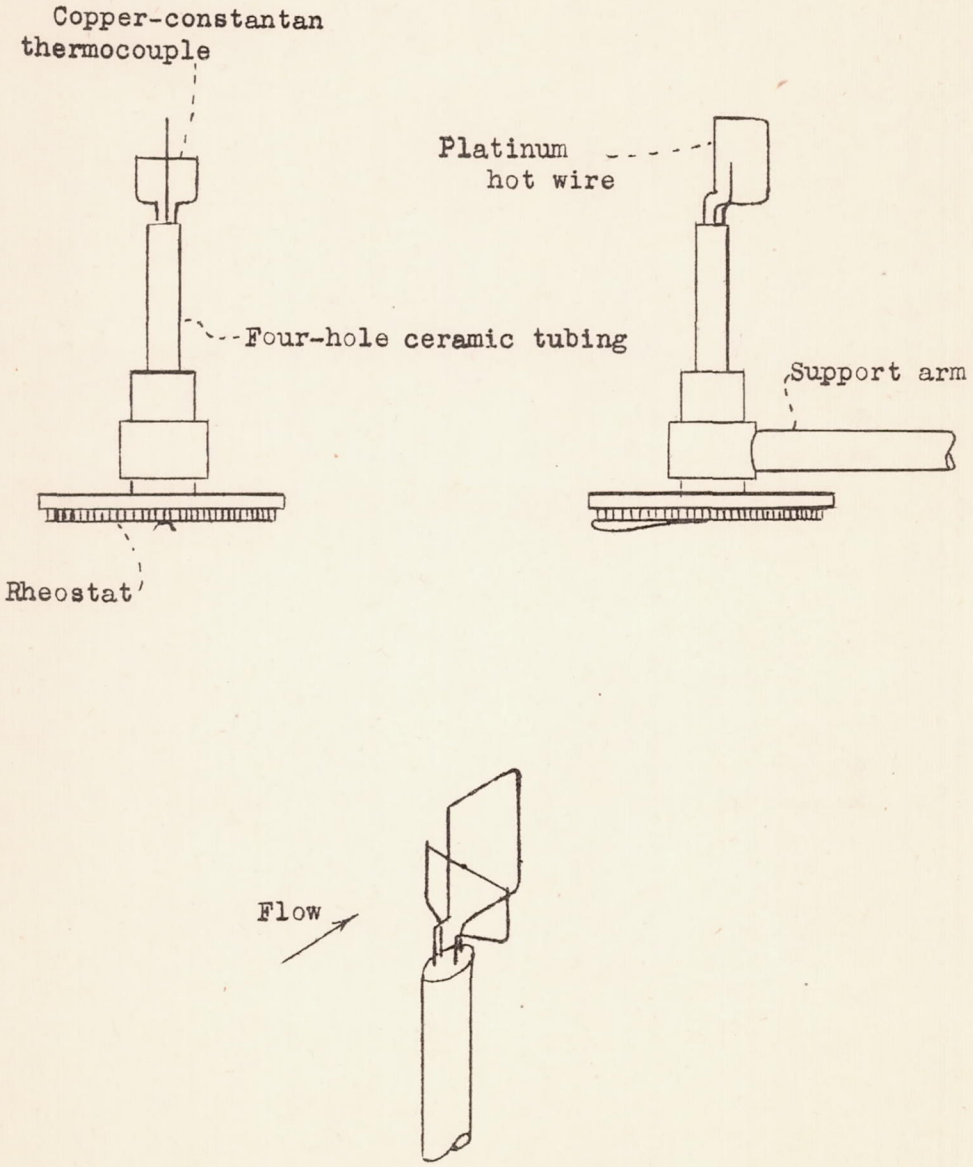

Figure 8.- Direction meter. Schematic sketch, not to scale. (Rotating drive not shown.)

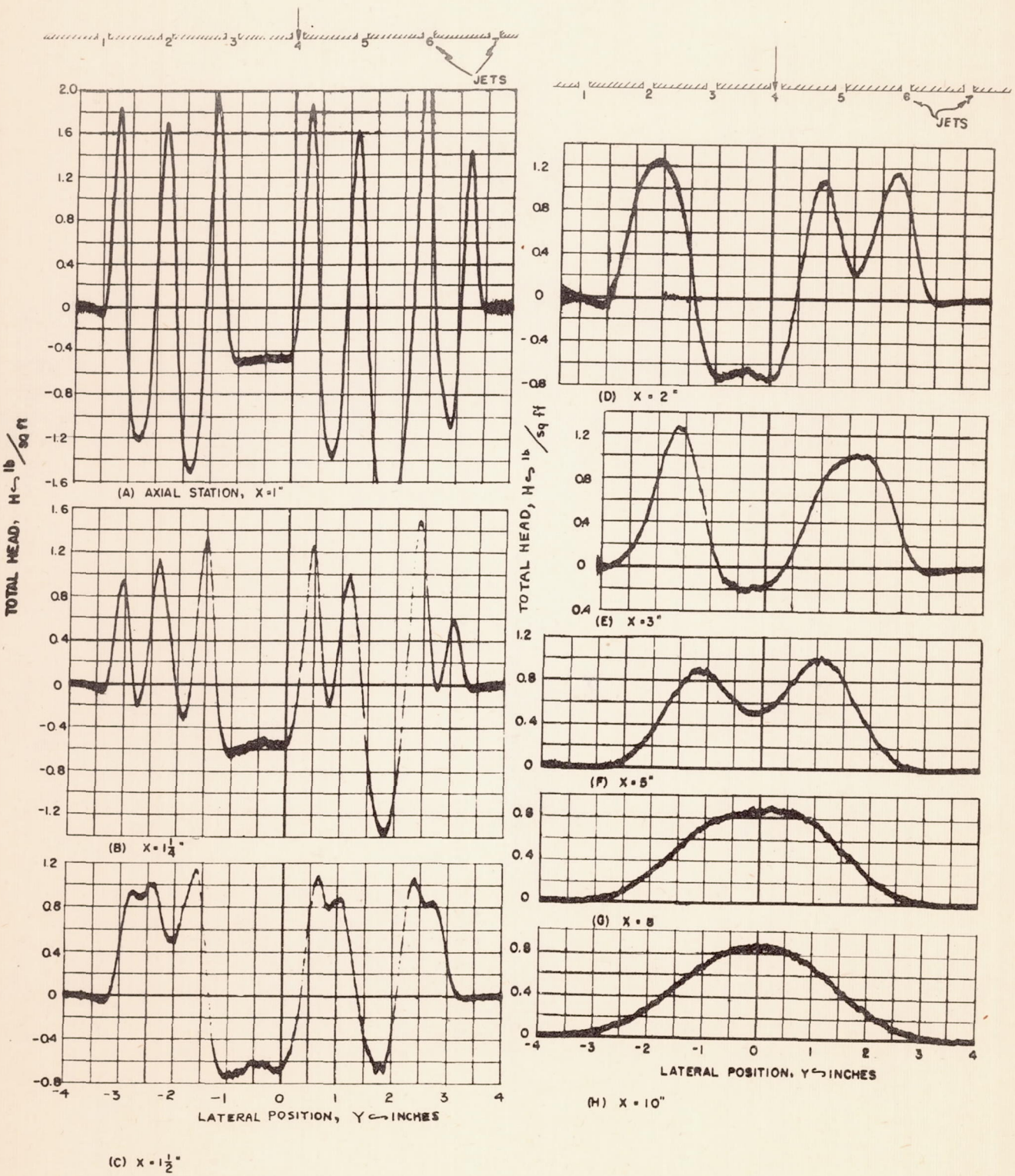

Figure 9.— Free jets. Lateral total-head distributions.

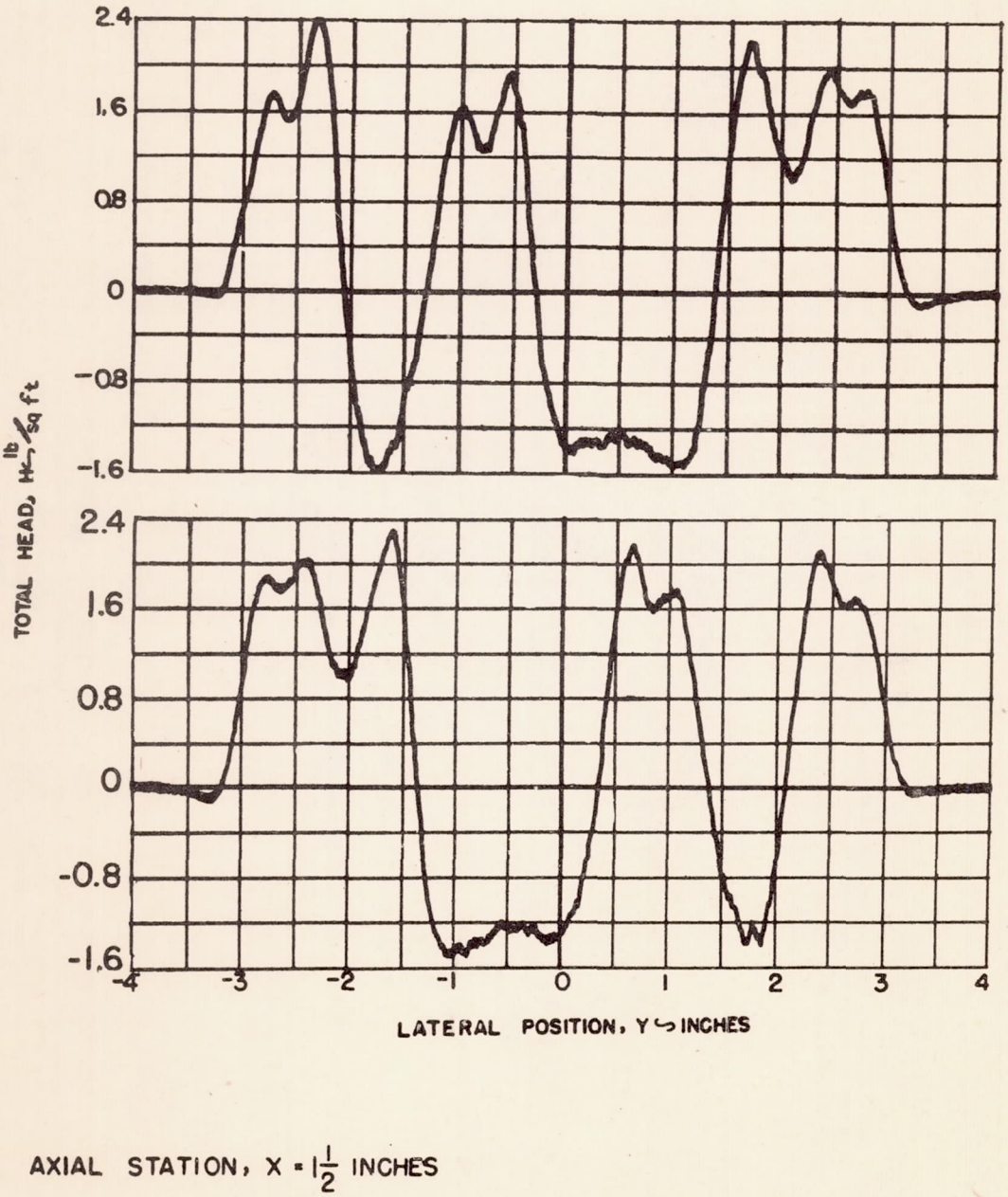

Figure 10.– Free jets. Alternative flow configurations resulting from instability.

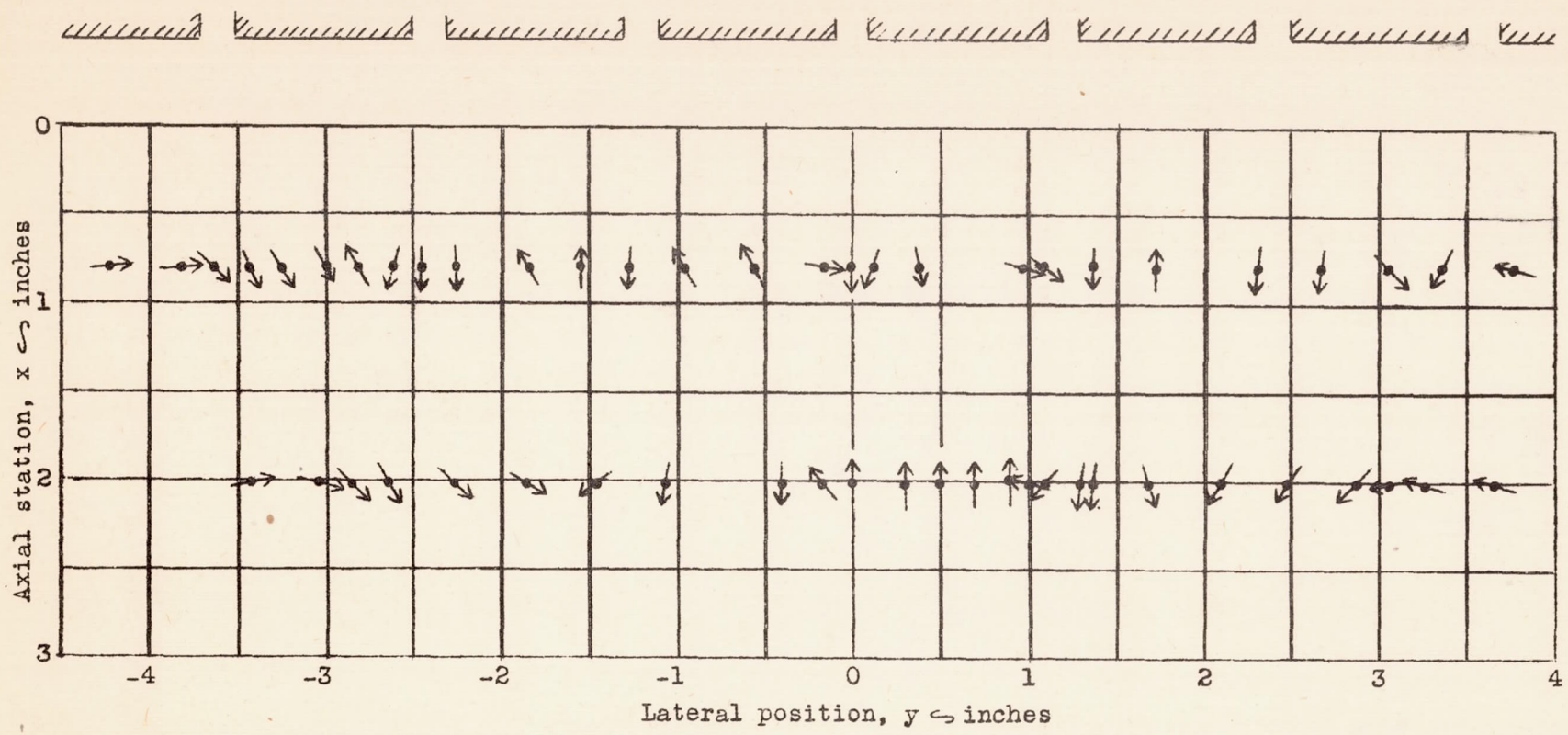

Figure 11.- Free jets. Direction of flow.

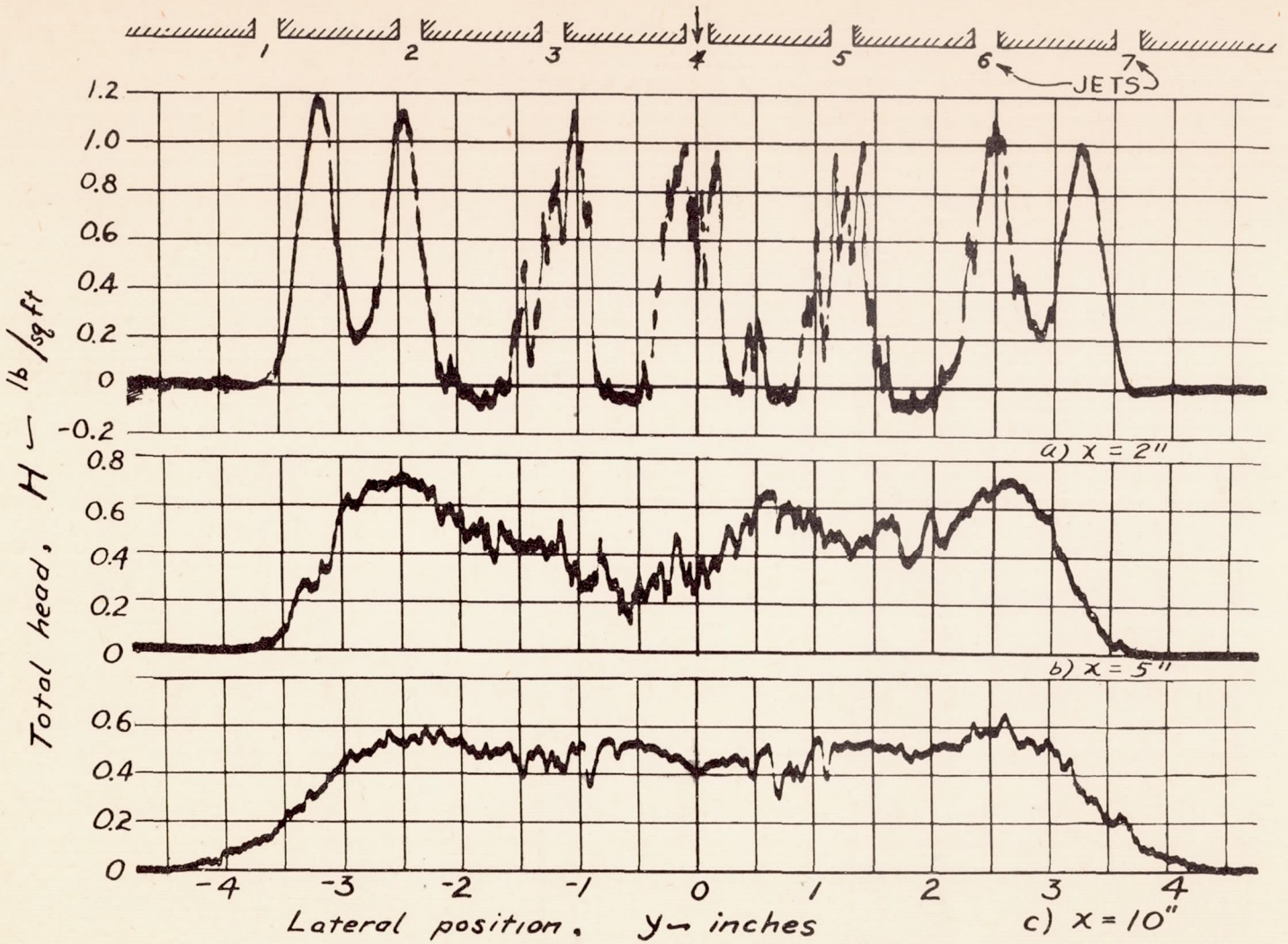

Figure 12.- Without end plates. lateral total-head distributions.

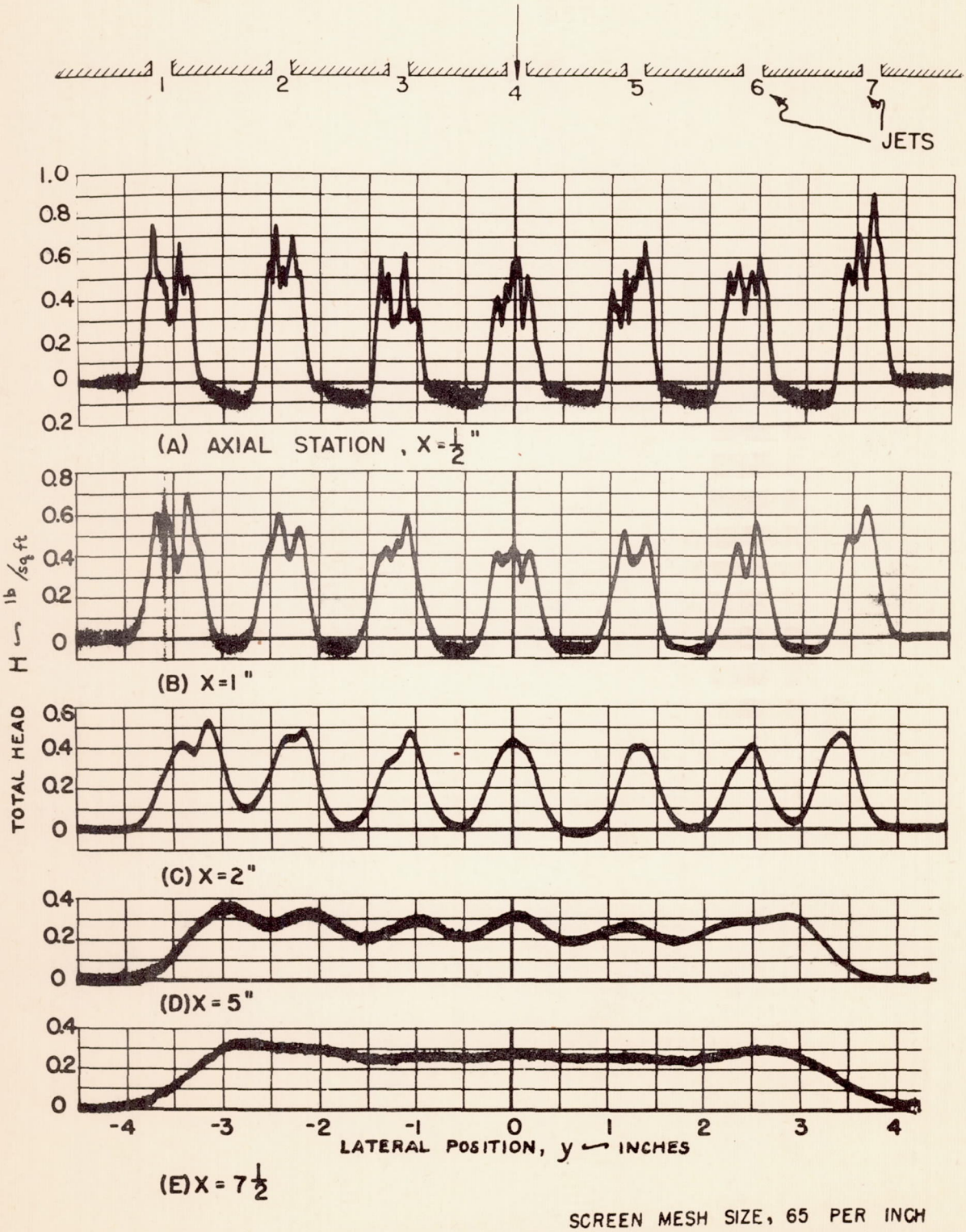

Figure 13.- Stabilizing effect of damping screen placed 1/4" downstream from slots. Lateral total-head distributions.

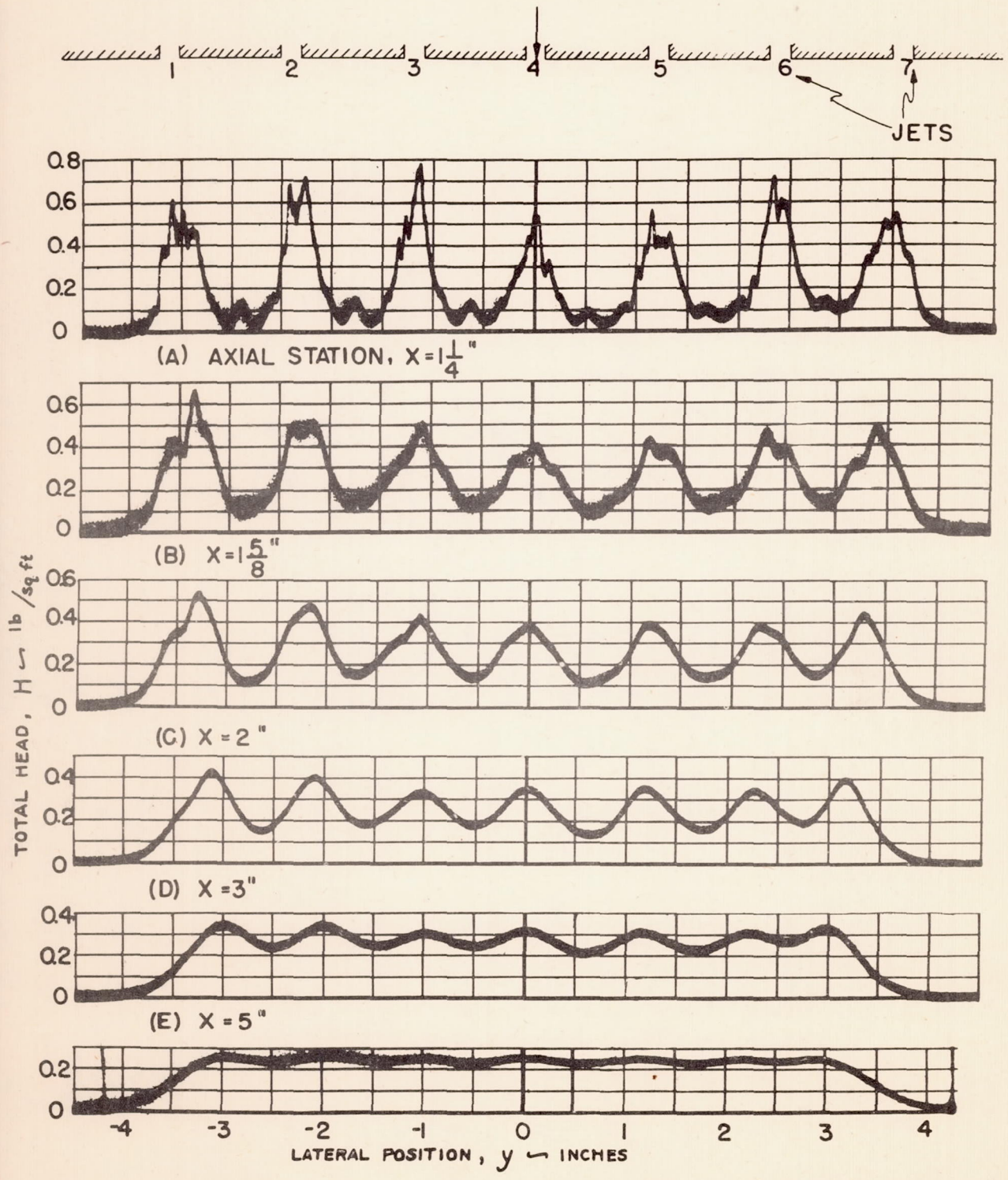

Figure 14.— Stabilizing effect of damping screen placed 1-1/16" downstream from slots. Lateral total-head distributions.

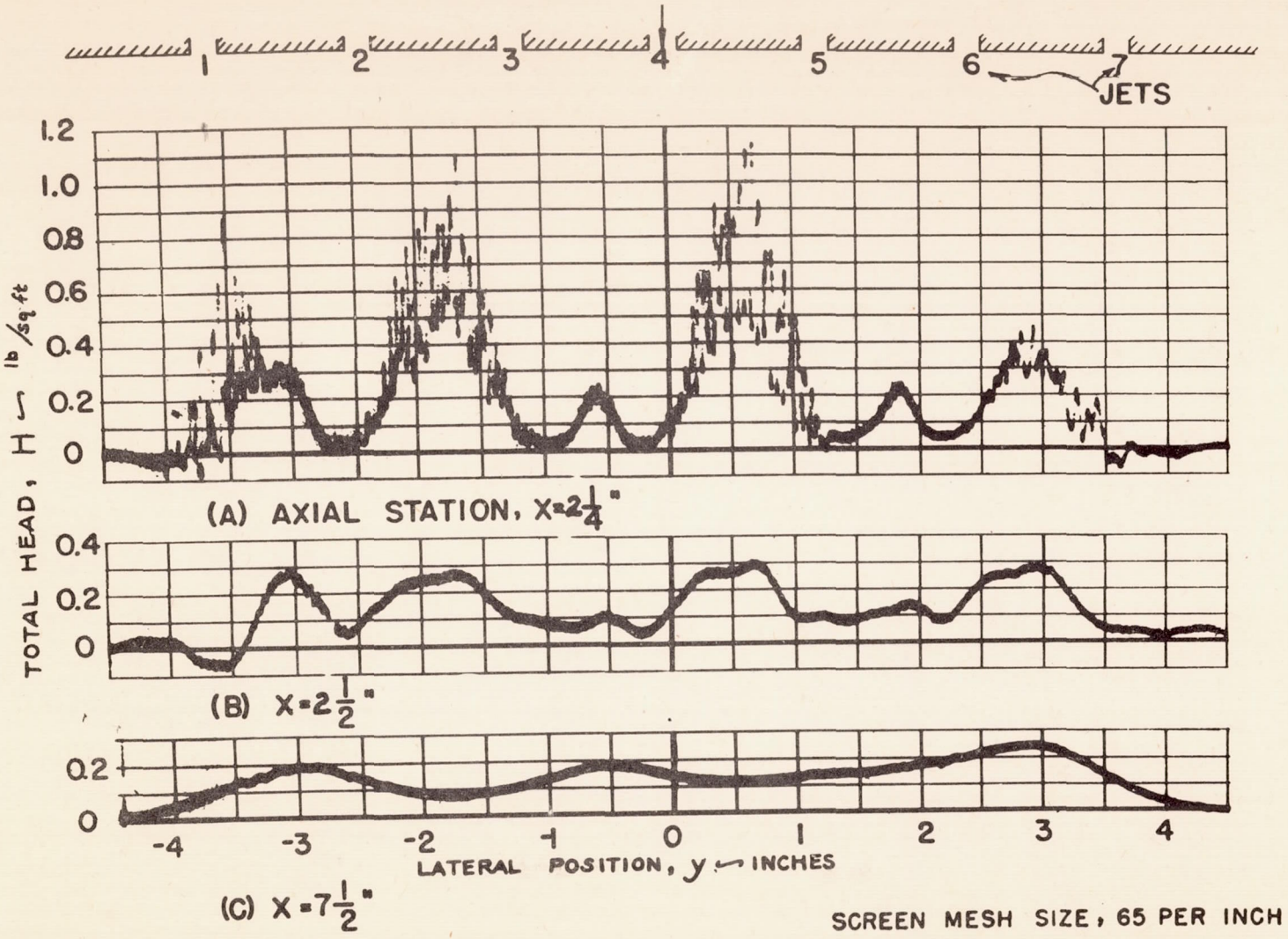

Figure 15.- Partial stabilizing effect of damping screen placed 2-1/8" downstream from slots. Lateral total-head distributions.

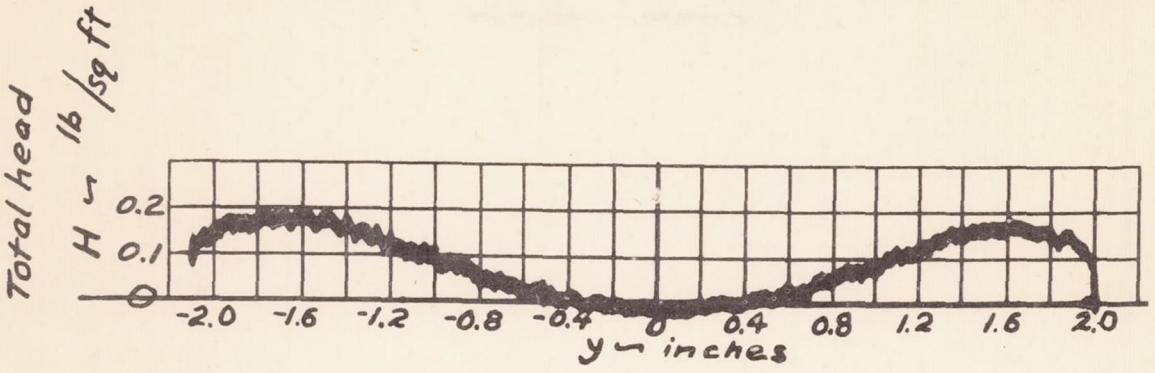

a) Contraction ratio = 2.0:1

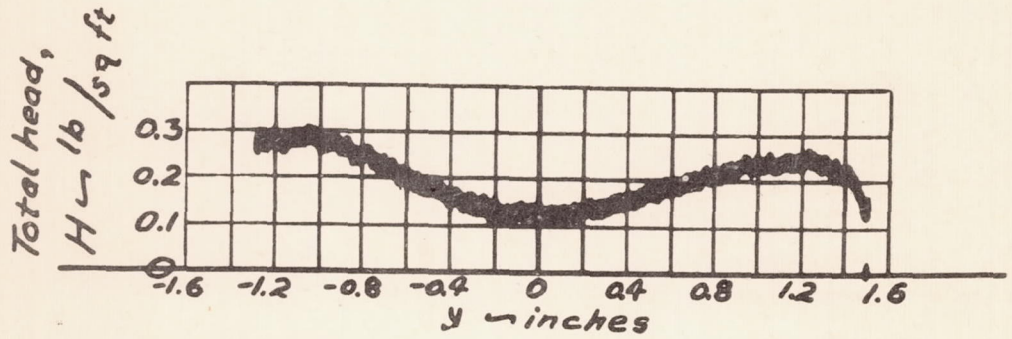

b) Contraction ratio = 2.7:1

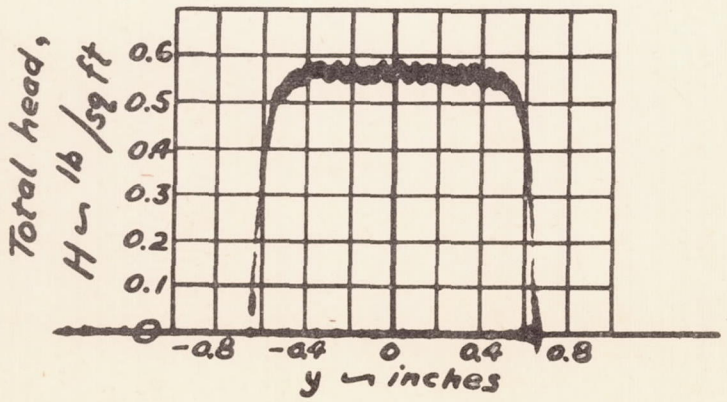

c) Contraction ratio = 6.7:1

All contraction wall radii = 11½ inches

Figure 16.- Effect of different downstream contractions. Total-head distribution at contraction throats.

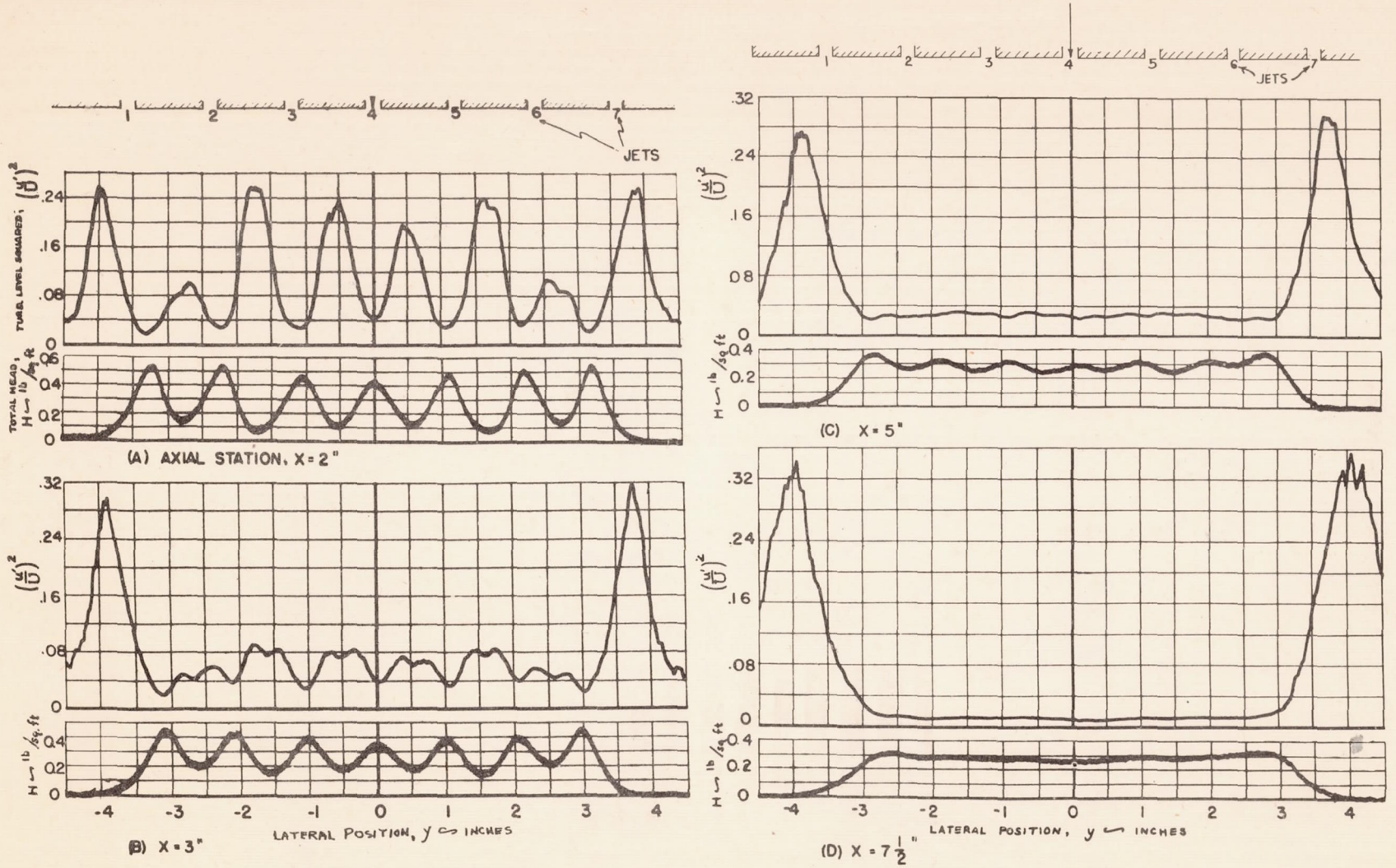

Figure 17.- Damping screen in stabilizing position (X = 1-1/4"). Lateral turbulence level and total-head distributions.

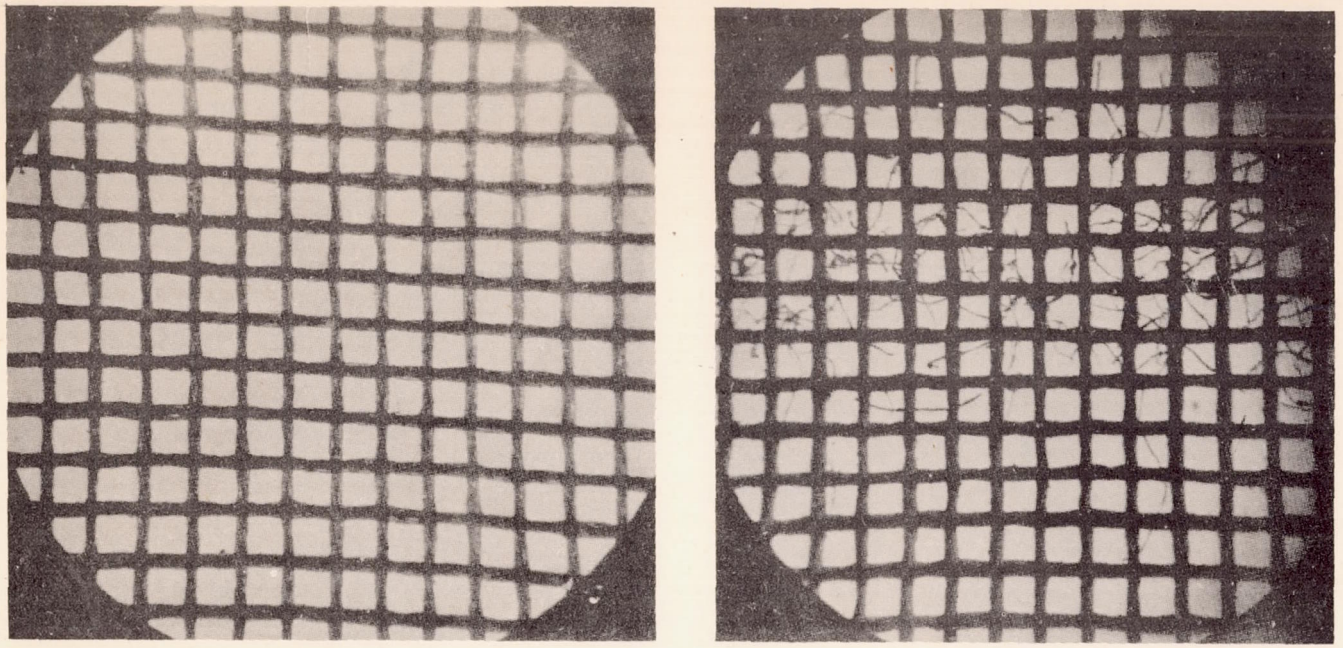

16 X

Clean Screen

Dusty Screen

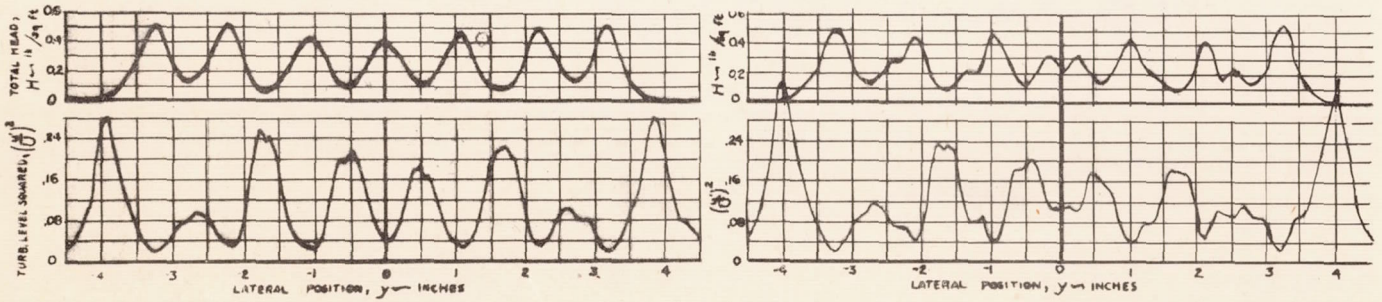

Figure 18.- Effect of dust in damping screen.

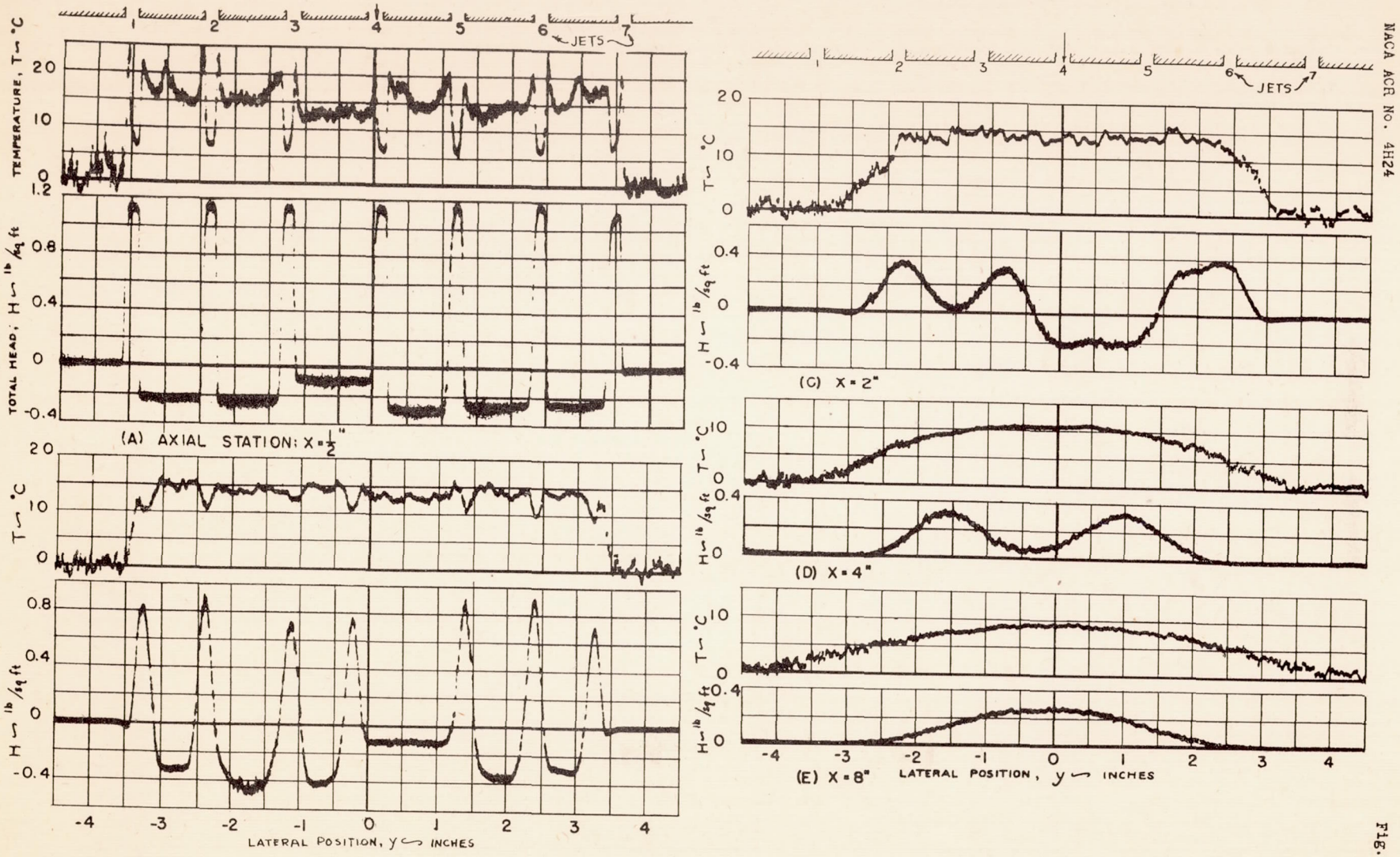

Figure 19.- Free jets. Lateral temperature and total-head distributions.

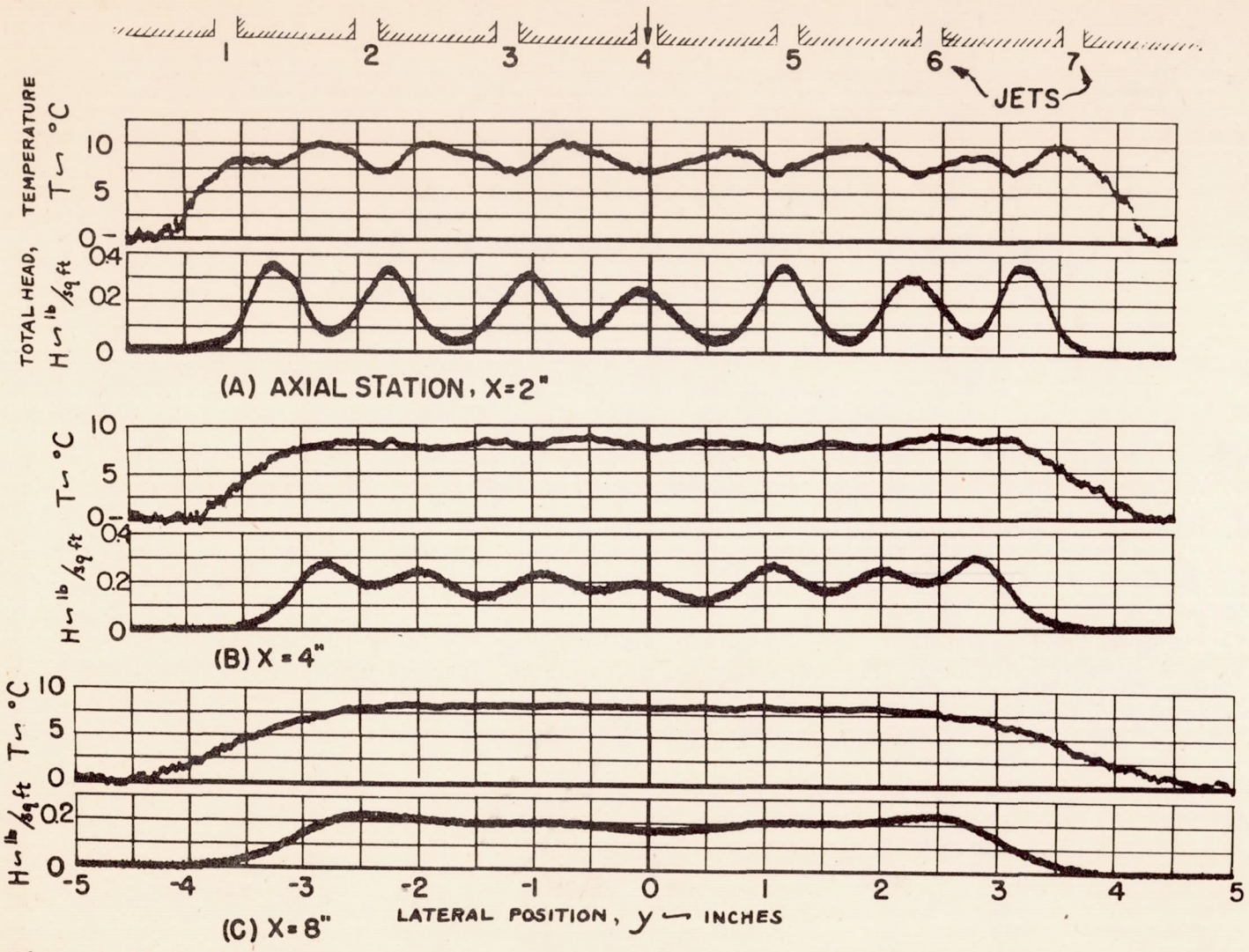

Figure 20.- Damping screen in stabilizing position (X_S = 1-1/4"). Lateral temperature and total head distributions.